Defective granulation tissue formation in mice with specific ablation of integrin-linked kinase in fibroblasts – role of TGFβ1 levels and RhoA activity

Katrin Blumbach[1,*], Manon C. Zweers[1,*], Georg Brunner[2], Andreas S. Peters[1], Markus Schmitz[1], Jan-Niklas Schulz[1], Alexander Schild[1], Christopher P. Denton[3], Takao Sakai[4], Reinhard Fässler[4], Thomas Krieg[1] and Beate Eckes[1,‡]

[1]Department of Dermatology, University of Cologne, Kerpener Strasse. 62, D-50937 Cologne, Germany
[2]Cancer Research, Fachklinik Hornheide, Münster 48157, Germany
[3]Centre for Rheumatology, Royal Free Hospital and University College London, London NW3 2QG, UK
[4]Molecular Medicine, Max-Planck Institute of Biochemistry, Martinsried 82152, Germany

*These authors contributed equally to this work
‡Author for correspondence (beate.eckes@uni-koeln.de)

Accepted 19 July 2010
Journal of Cell Science 123, 3872-3883

doi:10.1242/jcs.063024

Summary

Wound healing crucially relies on the mechanical activity of fibroblasts responding to TGFβ1 and to forces transmitted across focal adhesions. Integrin-linked kinase (ILK) is a central adapter recruited to integrin β1 tails in focal adhesions mediating the communication between cells and extracellular matrix. Here, we show that fibroblast-restricted inactivation of ILK in mice leads to impaired healing due to a severe reduction in the number of myofibroblasts, whereas inflammatory infiltrate and vascularization of the granulation tissue are unaffected. Primary ILK-deficient fibroblasts exhibit severely reduced levels of extracellular TGFβ1, α-smooth muscle actin (αSMA) production and myofibroblast conversion, which are rescued by exogenous TGFβ1. They are further characterized by elevated RhoA and low Rac1 activities, resulting in abnormal shape and reduced directional migration. Interference with RhoA–ROCK signaling largely restores morphology, migration and TGFβ1 levels. We conclude that, in fibroblasts, ILK is crucial for limiting RhoA activity, thus promoting TGFβ1 production, which is essential for dermal repair following injury.

Key words: Collagen-Cre, Focal adhesion, Mechanotransduction, Myofibroblast, Skin, Wound healing

Introduction

The interaction of cells with the surrounding extracellular matrix (ECM) is a key regulatory mechanism controlling essential cellular functions and differentiation (Cukierman et al., 2002; Humphries et al., 2004; Larsen et al., 2006). Fibroblasts are resident cells in connective tissues of various organs and are among the cells most intimately surrounded and controlled by ECM (Grinnell, 2003). Their phenotype is regulated by the biochemical composition of the matrix environment through signals transduced by specific integrin receptors, which are activated in response to matrix recognition (Hynes, 2002). Fibroblast–ECM crosstalk is mediated predominantly by the β1 subfamily of integrin receptors. These receptors are non-covalently associated transmembrane heterodimers that share the β1 subunit, which associates with any of 12 different α subunits. In skin, collagens represent the most abundant group of ECM macromolecules and, for their recognition, fibroblasts are equipped with three different β1 integrins (α1β1, α2β1 and α11β1) (Popova et al., 2007; Zhang et al., 2006a), endowing cells with a set of tools for finely tuned cellular responses and adaptation to challenges from outside.

Fibroblasts orchestrate the reconstitution of connective tissues following injury by inducing ECM synthesis, deposition and subsequent contraction of granulation tissue. To fulfill these tasks, fibroblasts can differentiate to myofibroblasts, which represent a specialized phenotype that is characterized by the expression and assembly of α-smooth muscle actin (αSMA) into thick stress fiber bundles (Hinz, 2007). Myofibroblasts occur transiently in healing wounds and pathologically in fibrotic conditions, in which they contribute to impaired organ function due to tissue contractures (Desmouliere et al., 2005; Gabbiani, 2003). Fibroblast to myofibroblast conversion is a stepwise process that is strictly dependent upon the contact of fibroblasts with the surrounding ECM, the generation of mechanical forces across focal adhesion structures and the presence of transforming growth factor beta-1 (TGFβ1) (Hinz, 2007; Kessler et al., 2001; Tomasek et al., 2002). When repopulating damaged connective tissue, fibroblasts first acquire an activated, migratory phenotype with de novo formation of stress fibers composed of cytoplasmic actin. These cells produce and remodel collagen, thereby further increasing mechanical tension across the cell membrane. In response to high local levels of TGFβ1 and to increasing mechanical tension in the wound ECM, activated fibroblasts express αSMA, which is assembled into stress fibers (Hinz, 2006; Shephard et al., 2004). This leads to substantially augmented contractile activity of fibroblasts, which are then termed myofibroblasts, and to tissue contraction (Hinz et al., 2001).

In mammals, three TGFβ isoforms exist, with TGFβ1 being a potent positive regulator of myofibroblast conversion. They are synthesized as large precursor polypeptides with the latency-associated peptide (LAP) at the N terminus and the TGFβ peptide at the C terminus. In the endoplasmic reticulum, furin cleaves pro-TGFβ and induces formation of the small latent TGFβ complex, in which TGFβ remains non-covalently associated with its propeptide, LAP, and unable to bind to its receptors. The small latent complex might be further linked via LAP to latent TGFβ-binding proteins

(LTBPs), giving rise to the large latent TGFβ complex. After secretion, the LTBPs target the large latent TGFβ complex to binding sites in the extracellular matrix, such as fibronectin or fibrillin-1. Thus, large amounts of TGFβ are stored in latent form in tissues (reviewed by Sheppard, 2006). Activation and release of bioactive TGFβ must be under tight control in view of its potent and pleiotropic effects. Different mechanisms have been described, including in vitro activation by extremes of temperature or pH. In vivo, thrombospondin-1 contributes to activation of TGFβ1 by binding to LAP and inducing a conformational rearrangement such that LAP cannot confer latency on the mature domain of TGFβ1 (Crawford et al., 1998; Murphy-Ullrich and Poczatek, 2000). Interestingly, integrins have turned out to be important players in latent TGFβ activation (Annes et al., 2004; Munger et al., 1999; Aluwihare et al., 2009; Mu et al., 2002; Sheppard, 2005).

In addition to the presence of TGFβ1, myofibroblast formation requires the transmission of mechanical stress to the fibroblast cytoskeleton across properly structured force-bearing matrix adhesions (Hinz, 2006). These consist of ECM ligands bound to integrins, which are organized into clusters, called focal adhesions (FAs), with the cytoplasmic tails of β1 subunits binding to a large submembranous complex of proteins containing talin, vinculin, paxillin, tensin, focal adhesion kinase, integrin-linked kinase (ILK) and many others (Cukierman et al., 2002; Hinz, 2006; Sawada and Sheetz, 2002; Thannickal et al., 2003). ILK is a scaffolding molecule that connects the intracellular domains of β1 and β3 integrin subunits to further bridging molecules (Hannigan et al., 1996; Nikolopoulos and Turner, 2001; Tu et al., 2001; Yamaji et al., 2001; Rosenberger et al., 2003). It supplies a structural platform linking ECM-bound integrins to actin cables and integrates several signaling pathways that regulate cell behavior (reviewed by Legate et al., 2006).

Actin organization and cell contractility are linked to transforming protein RhoA (Nobes and Hall, 1999; Chrzanowska-Wodnicka and Burridge, 1996). In muscle and non-muscle cells such as fibroblasts, RhoA signals via Rho-associated kinase (ROCK) to phosphorylate myosin light chain (MLC) and to inhibit MLC phosphatase. This is associated with increased cell contractility. Early phases of cell spreading are characterized by high activity of the RhoA-related GTPase Rac1, which facilitates spreading and lamellipodium formation, and concomitant suppression of RhoA activity by Rac1 (Sander et al., 1999).

Constitutive ablation of ILK function in mice results in peri-implantation lethality as a result of adhesion and polarization defects of the epiblast (Sakai et al., 2003). More recently, ILK inactivation has been targeted conditionally to selected cell types (Lorenz et al., 2007; Nakrieko et al., 2008; Gheyara et al., 2007; White et al., 2006; Grashoff et al., 2003). Common to all mutants, including the constitutively ablated early embryo, is the formation of sparse, short or condensed actin filaments, abnormal cell shape and dysregulated cell proliferation, which is either augmented or repressed, depending on the affected cell type.

We targeted ILK inactivation to fibroblasts in the skin of young mice to test the hypothesis that ILK maintains a crucial function as a docking structure in FAs connecting the ECM with the actin cytoskeleton. We report that myofibroblast formation is strongly impaired, leading to diminished dermal tissue repair in vivo. Primary ILK-deficient skin fibroblasts reveal an abnormal shape, enhanced RhoA activity, reduced TGFβ1 and αSMA production, and delayed directed migration. These defects were rescued by interfering with RhoA–ROCK signaling, indicating that, in fibroblasts, ILK limits RhoA activity.

Results

Efficient deletion of ILK in skin fibroblasts in vivo and in vitro

Targeting of ILK inactivation to fibroblasts was accomplished using a mouse strain carrying the Cre–ER^{T} fusion transgene under the control of a minimal collagen α2 type I promoter and enhancer driving fibroblast-specific and inducible Cre expression (Fig. 1A) (Sonnylal et al., 2007; Zheng et al., 2002). These mice were crossed to mice in which both *Ilk* alleles were mutated by the insertion of *loxP* sites flanking exon 2 (homozygous *Ilk*$^{fl/fl}$) (Grashoff et al., 2003) to produce compound ILK$^{fl/fl}$; Cre-positive animals (Fig. 1B). Littermate animals of the genotypes *Ilk*$^{fl/+}$; *Cre*^{pos}, *Ilk*$^{fl/+}$; *Cre*^{neg} or *Ilk*$^{fl/fl}$; *Cre*^{neg} were used as controls. Cre activity was induced in all animals including controls at 12 days of postnatal life by intraperitoneal administration of tamoxifen for five consecutive days as previously described (Zheng et al., 2002; Liu et al., 2009; Sonnylal et al., 2007). Induction of Cre activity was examined in parallel experiments, in which the collagen Cre line was mated to reporter mice harboring a *lacZ* gene encoding β-galactosidase that was interrupted by a *loxP*-flanked stop cassette (Soriano, 1999). Cre activity was confirmed by blue staining in the granulation tissue at 7 days after injury, leaving the epidermis unaffected (supplementary material Fig. S1).

Absence of ILK was confirmed in primary fibroblasts isolated from the dermis of tamoxifen-treated mice at 3 weeks of age by immunofluorescence (Col1-ILK; Fig. 1C) and western blot analysis (fl/fl Cre; Fig. 1D). Abundant ILK expression and partial localization in focal adhesion sites was detected in control cells, whereas deleted cells were negative. Very rarely, some deleted fibroblasts exhibited ILK expression (Fig. 1C,D), indicating highly efficient but not complete induction of Cre recombinase activity and ILK deletion in all skin fibroblasts.

Reduced granulation tissue formation and contraction in Col1-ILK mice

By clinical inspection, the skin of Col1-ILK mice appeared inconspicuous before and directly after tamoxifen administration. In addition, histological analysis of the unwounded skin from these mice did not reveal histomorphological differences from controls (supplementary material Fig. S2). We then challenged the animals after tamoxifen administration by creating full-thickness wounds on their backs as previously described (Zweers et al., 2007). Cross-sections taken from the center of wounds at 7 days after injury revealed complete re-epithelialization in all animals. There was a tendency towards acanthosis in control wounds but, overall, the overlying neo-epidermis appeared normal (Fig. 2A). By contrast, granulation tissue formation was severely reduced in wounds of mutant animals (Fig. 2A, lower panel), resulting in greater wound width (Fig. 2A, lower panel, and Fig. 2B) and less granulation tissue (Fig. 2C). Routine histology also indicated markedly reduced cellularity in the granulation tissue, whereas blood vessel numbers appeared unaltered. Moreover, immunostaining revealed normal abundance of macrophages (F4/80 staining, not shown). Myofibroblasts in the granulation tissue were visualized by staining for αSMA, which was detected in the smooth muscle layer of blood vessels in control and mutant wounds (Fig. 2D, arrows). However, myofibroblasts were virtually absent in wounds of Col1-ILK mice, whereas abundant myofibroblasts were observed in control wounds (Fig. 2D, arrowheads). Ki67 staining revealed reduced numbers of proliferating cells in the dermis of mutant mice (Fig. 2E,F).

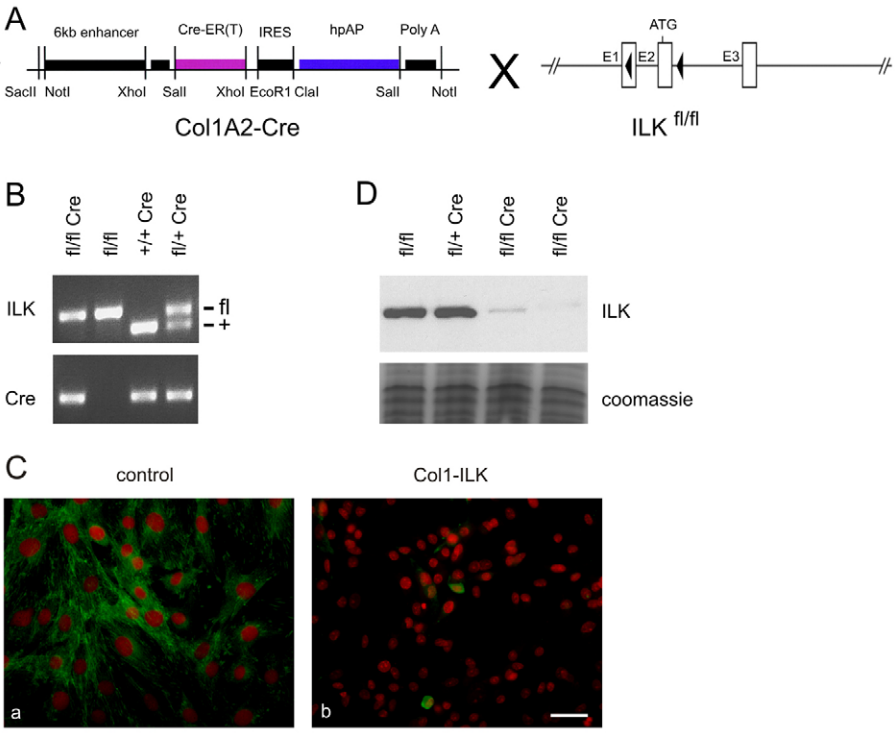

Fig. 1. Targeted inactivation of ILK in fibroblasts. (**A**) Schematic of relevant elements of the *Col1a2–Cre* locus (left) (Zheng et al., 2002) and the floxed *Ilk* construct (Grashoff et al., 2003). (**B**) Representative genotype analysis by PCR of DNA from tail biopsies showing the floxed (fl) or wild type (+) (top) and presence of *Cre* allele (bottom). (**C**) Absence of ILK was verified in primary fibroblasts isolated from the dermis of Col1-ILK mice after tamoxifen administration. Control fibroblasts displayed abundant ILK expression (green), which was partially localized in matrix adhesions. Nuclei were stained with propidium iodide. Cells were grown on tissue culture plastic for 24 hours in DMEM supplemented with 10% FCS. Scale bar: 50 μm. (**D**) ILK deletion in fibroblasts was verified by western immunoblotting of protein extracts of primary fibroblasts isolated from the dermis of mice.

Interestingly, the number of Ki67-positive keratinocytes in the basal layer of mutant epidermis also appeared to be lower, suggesting an altered epithelial–mesenchymal crosstalk.

Impaired myofibroblast formation in response to mechanical activation

To determine the mechanisms leading to reduced myofibroblast numbers in mutant wounds and to delineate cell-autonomous effects, we characterized primary fibroblasts that were isolated from the dermis of Col1-ILK and control mice at ~3 weeks after birth, which was around 2–5 days after the last injection with tamoxifen.

To explain the striking absence of myofibroblasts in mutant granulation tissue, we first tested proliferative potential; however, no significant differences were observed in vitro in monolayer cultures (supplementary material Fig. S3A) or in tethered three-dimensional collagen lattices (supplementary material Fig. S3B). We then examined the capacity of ILK-deficient fibroblasts to differentiate to myofibroblasts in vitro, using tethered collagen lattices in which fibroblasts develop forces counterbalancing stress from an ECM environment under tension (Kessler et al., 2001; Tomasek et al., 2002). Fibroblast to myofibroblast conversion was determined by analyzing αSMA expression as the hallmark of myofibroblasts. In comparison with controls, ILK-deficient fibroblasts showed sharply reduced αSMA signals (Fig. 3A).

Because TGFβ1 is a potent inducer of αSMA, we next tested whether reduced formation of myofibroblasts might result from reduced TGFβ1 activity produced by ILK-deficient fibroblasts. Reverse transcription (RT)-PCR and northern blot hybridization revealed similar *Tgfb1* mRNA levels (Fig. 3B). We then assessed levels of total (i.e. latent and active, measured following heat activation) and active TGFβ1 protein in the supernatant of fibroblasts cultured in tethered collagen lattices. The assay made use of mink lung epithelial cells, which are engineered to express luciferase driven by the TGFβ1-responsive plasminogen activator inhibitor-1 (PAI-1) promoter (Abe et al., 1994). In contrast to comparable *Tgfb1* mRNA levels, amounts of both total and active TGFβ1 protein present in conditioned medium were significantly lower in *Ilk*-null fibroblasts than in controls (Fig. 3C). The fraction of active TGFβ1 was similar in mutant (19% of total) and control (20% of total) fibroblasts.

Rescue of αSMA production and myofibroblast formation by exogenous TGFβ1

Apparently, the levels of fibroblast-generated TGFβ1 were not sufficient to induce the myofibroblast phenotype in vitro. To determine whether ILK-deficient fibroblasts are able to respond to exogenously added TGFβ1 in vitro and which functions might be restored, we assessed selected fibroblast properties and functions in cells grown with 10 ng/ml TGFβ1 in medium supplemented with 1% fetal calf serum (FCS). TGFβ1 signaling was activated in both control and ILK-deficient fibroblasts, as confirmed by phosphorylation of Smad2 (Fig. 4A). Levels of phosphorylated Smad2 were comparable after stimulation with exogenous TGFβ1, indicating that TGFβ receptors are normally expressed and functional on mutant cells. Western blot analysis and quantification of signals demonstrated that supplying exogenous TGFβ1 to ILK-deficient fibroblasts resulted in restoration of αSMA expression to control levels (Fig. 4A). Rescue was confirmed by immunofluorescence analysis using antibodies directed against αSMA. Without TGFβ1, ILK-deficient fibroblasts displayed few αSMA-positive stress fibers, if any (Fig. 4B), whereas addition of TGFβ1 resulted in incorporation of αSMA into clearly visible stress fibers in all ILK-deficient fibroblasts.

The larger wound size of Col1-ILK mice further suggests that mutant fibroblasts are less able than wild-type controls to contract collagen matrices. This defect was indeed observed and was largely rescued by addition of exogenous TGFβ1 (Fig. 4D).

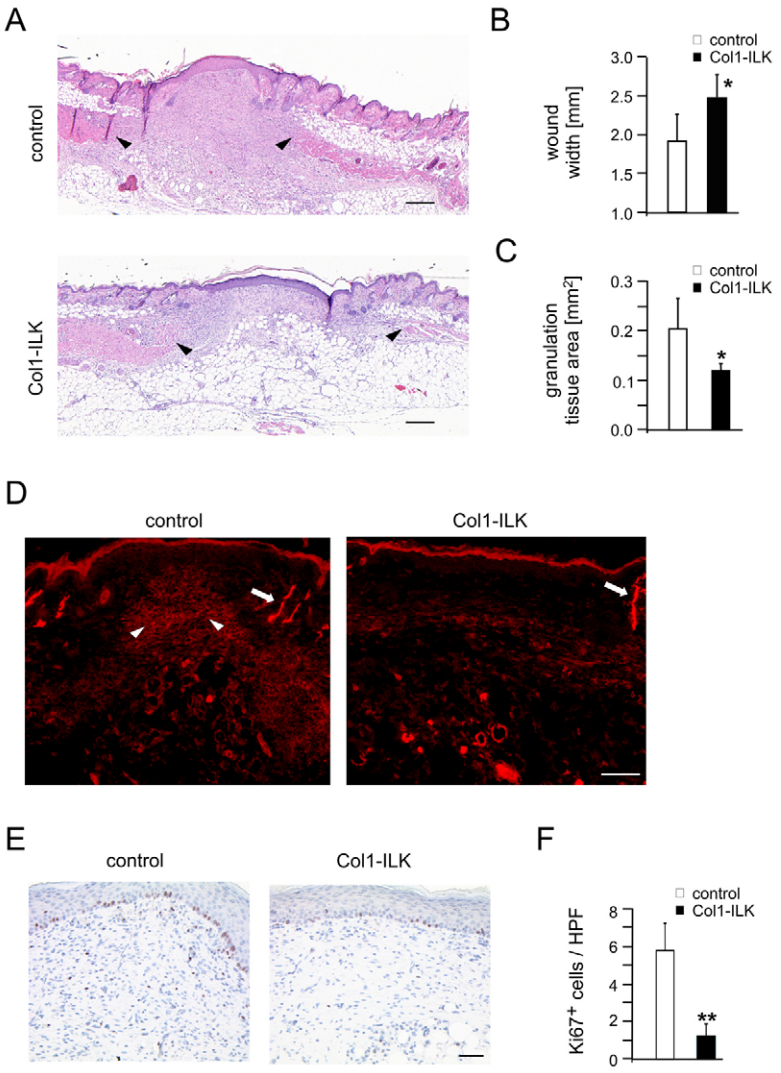

Fig. 2. Reduced dermal wound healing in Col1-ILK mice at 7 days after wounding. (**A**) Histology of wound sections taken from the center of wounds at 7 days after injury and stained with H&E. Wounds in both genotypes are covered by new epidermis, but formation of the underlying granulation tissue is strongly impaired in Col1-ILK mice. (**B**) Significantly wider wounds are due to reduced wound contraction (P<0.05), as assessed by the distance between the cut margins of the panniculus carnosus muscle (indicated by arrowheads in A). (**C**) A significantly smaller area (mm^2) is filled by granulation tissue in wounds of Col1-ILK mice (P<0.05). (**D**) Sections from the wound centers were incubated with antibodies recognizing αSMA in smooth muscle cells of blood vessels (arrows) and myofibroblasts in the granulation tissue of control wounds (arrowheads). (**E**) Immunohistochemical staining of Ki-67 illustrating proliferating cells (brown color). (**F**) Numbers of Ki67-positive cells are significantly reduced in the dermal compartment of Col1-ILK wounds compared with controls, as assessed by counting of cells in five high-power fields (**P<0.01; n=6–10 animals per genotype). Error bars indicate s.d. Scale bars: 200 μm (A) and 50 μm (D,E).

Cell morphology and matrix adhesion architecture are not restored by exogenous TGFβ1

Microscopic inspection of cultured fibroblasts displayed striking differences in cell shape: cells derived from Col1-ILK skin were thin and spread mostly to a needle-like shape (Fig. 5). This morphological difference was observed on integrin β1 substrates, including collagen I (Fig. 5A) and fibronectin (Fig. 5B), and on vitronectin, an integrin β3 substrate (supplementary material Fig. S4). Reduced spreading might be accounted for by reduced surface expression of integrin receptors; however, expression analysis of integrin subunits β1, α2, α5 and αvβ3 by flow cytometry did not reveal significant differences between *Ilk*-null and control fibroblasts and thus ruled out this explanation (data not shown). Furthermore, no differences in integrin conformation and, hence, ligand affinity and activation status were observed, as indicated by unaltered needle-shaped morphology of mutant fibroblasts upon spreading in medium containing magnesium (supplementary material Fig. S4 and data not shown).

In addition to abnormal cell shape, ILK-deficient fibroblasts failed to organize F-actin filaments in a manner similar to that of controls (Fig. 5A, top panel). Vinculin-positive matrix adhesions in mutant cells appeared shorter and thicker (Fig. 5A, middle panel and insets), and their number was lower than controls (22 per *Ilk*-null cell versus 91 per control cell; n=100 cells per genotype), indicating disrupted architecture of actin microfilaments and matrix adhesions. In contrast to the restorative effect of exogenous TGFβ1 on αSMA expression, no rescue of cell shape was observed upon treating ILK-deficient fibroblasts with TGFβ1. Abnormal shape and organization of F-actin and matrix adhesions were most pronounced in the early post-adhesion phase, where ILK deficiency clearly resulted in failure of cells to spread (Fig. 5B). Here, phalloidin staining for F-actin revealed a broad, condensed band of cortical actin at the cell periphery and short cytoplasmic cables in fibroblasts lacking ILK. In addition, vinculin was localized diffusely and only occasionally associated with very faint small, rod-like structures at the cell periphery.

Increased RhoA activity as a cause of aberrant fibroblast morphology

The persistence of altered size and shape of ILK-deficient fibroblasts following TGFβ1 treatment suggested the involvement of further mechanisms in cell-shape determination. In particular, the sharply reduced cell size and actin filament arrangement in deficient fibroblasts that was detected after 2 hours of culture raised the question whether the cells might be unable to spread owing to insufficient amounts of active Rac1 and concomitantly

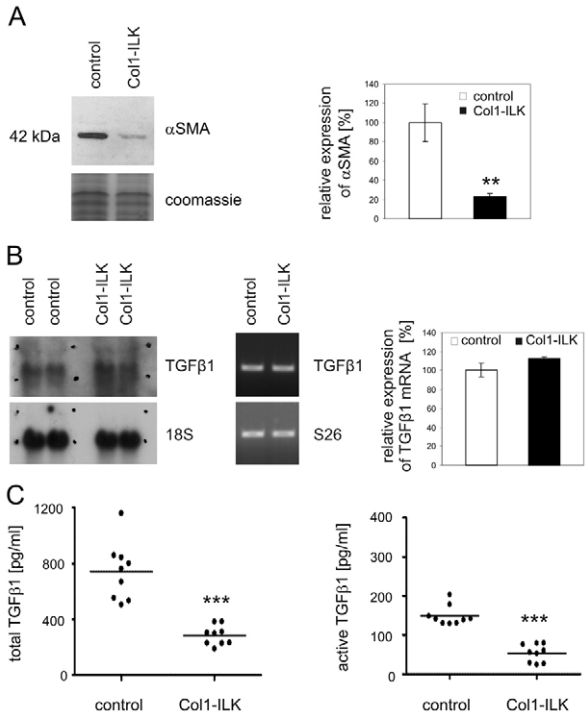

Fig. 3. Impaired αSMA production and reduced levels of secreted and active TGFβ1 in ILK-deficient fibroblasts. Cells were grown for 24 hours in tethered collagen lattices. (**A**) Western blot shows significantly diminished levels of αSMA in ILK-deficient fibroblasts (P=0.002; n=3). (**B**) Northern blot of RNA from ILK-deficient and control fibroblasts, hybridized to a ^{32}P-dCTP-labeled cDNA probe for murine *Tgfb1*, indicates similar *Tgfb1* steady-state transcript levels (left panel). Similar *Tgfb1* mRNA levels were also detected by semi-quantitative RT-PCR, normalized to levels of S26 mRNA (middle panel). Quantification of RT-PCR signals did not reveal significant differences (P>0.05; n=4). (**C**) Levels of total and active TGFβ1 present in lattice supernatants were analyzed using mink lung epithelial cells, showing significantly reduced levels of both in ILK-deficient fibroblast cultures (P<0.0001). Error bars are ± s.d.

elevated RhoA activity. To address this question, we first incubated ILK-deficient and control fibroblasts with Y-27632, which interferes with RhoA signaling by inhibiting ROCK. First, starved cells were seeded for 2 hours in the presence of 5 μM Y-27632 onto fibronectin-coated glass surfaces. Previous results have shown that enhanced spreading by *Ilk*-null fibroblasts following treatment with inhibitor was most pronounced at 2 hours after addition of the inhibitor and lasted until a maximum of 6 hours (K.B., data not shown). Phase-contrast images show a clear effect with relaxation and enhanced spreading of ILK-deficient fibroblasts (Fig. 6A). Quantification of the cell area at 2 hours after seeding revealed that untreated *Ilk*-null fibroblasts covered 44% of the area covered by controls (Fig. 6B; P<0.0001; n>224). Rho–ROCK inhibition resulted in expansion of ILK-deficient fibroblasts to 75% relative to untreated controls (P<0.0001; n>224). Parallel cultures were incubated with TGFβ1 (data not shown), which resulted in expansion to 56%: a modest increase in spreading of ILK-deficient fibroblasts in comparison with the area covered by controls, confirming our previous results, indicating that TGFβ1 is unable to normalize cell shape (Fig. 5). To examine the effects of Rho–ROCK inhibition on cells that were already fully spread, we also treated cultures at 24 hours after seeding with Y-27632 for 2 hours

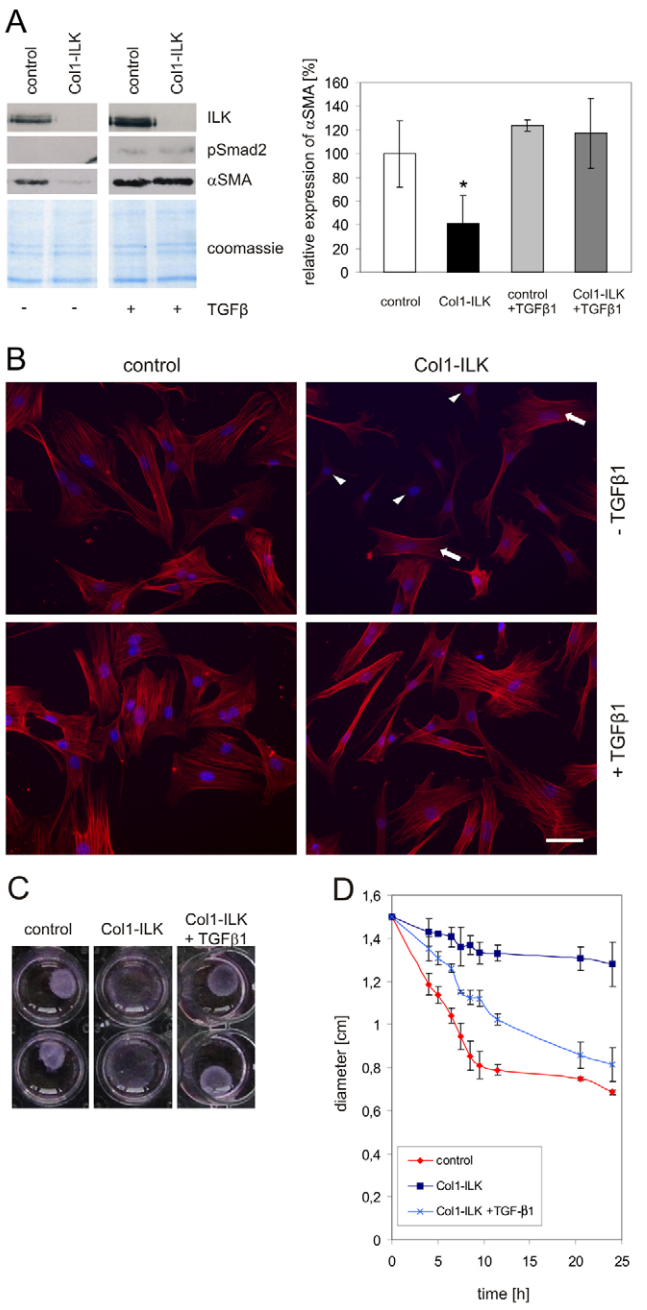

Fig. 4. Rescue of αSMA production by exogenous TGFβ1. ILK-deficient and control fibroblasts were starved overnight in 1% FCS, then grown for 24 hours in 1% FCS with or without 10 ng/ml of TGFβ1. (**A**) Western blot of cell extracts showing expression of ILK and αSMA. TGFβ1-dependent signaling was assessed by probing extracts for phosphorylated Smad2 (pSmad2). Quantification by densitometry shows significant differences in αSMA production by untreated ILK-deficient fibroblasts (P<0.05; n=4), which are abolished by TGFβ1 treatment. (**B**) Visualization of αSMA-positive stress fibers in fibroblasts grown on tissue culture plastic with or without 10 ng/ml TGFβ1. Arrowheads indicate ILK-deficient fibroblasts not expressing αSMA. Arrows indicate ILK-deficient fibroblasts that are positive for αSMA, but failed to incorporate αSMA into stress fibers. Nuclei are counterstained with DAPI (blue). Scale bar: 50 μm. (**C**) Reorganization of collagen fibers by ILK-deficient and control fibroblasts, grown for 24 hours in floating collagen lattices with or without 10 ng/ml TGFβ1. A representative of n=4 experiments is shown. (**D**) Reduction in lattice diameter (cm) over 24 hours. Error bars are ± s.d.

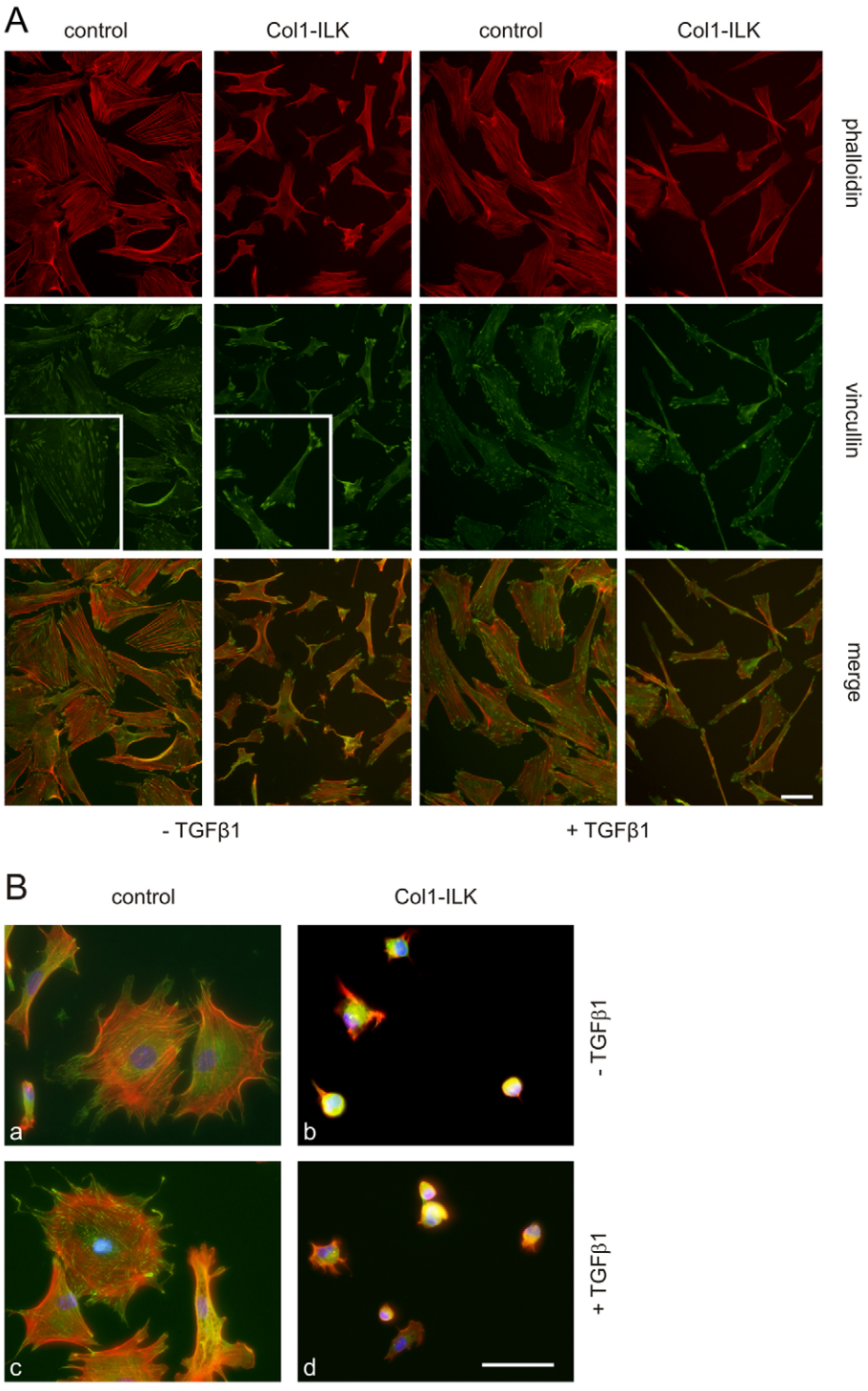

Fig. 5. Abnormal morphology and impaired spreading of ILK-deficient fibroblasts. Morphology of ILK-deficient and control fibroblasts grown on glass-bottom chamberslides coated with collagen I (**A**) or fibronectin (**B**). Visualization of F-actin organization (phalloidin in red) and focal adhesions (vinculin in green). (A) Fibroblasts were starved overnight in 1% FCS, then grown for 24 hours in DMEM with 1% FCS with or without 10 ng/ml TGFβ1. Insets in the vinculin panel show appearance of focal adhesions at higher magnification. (B) Morphology of control (a,c) and ILK-deficient fibroblasts (b,d) grown for 2 hours on glass-bottom chamberslides coated with fibronectin in the absence (a,b) or presence (c,d) of 10 ng/ml TGFβ1. ILK-deficient fibroblasts are poorly spread, F-actin (red) is organized in a dense cortical band but not in stress fibers and vinculin (green) is not organized in focal contacts. In control cells, by contrast, stress fibers are present, which terminate in well-demarcated focal contacts. Nuclei are counterstained with DAPI (blue). Scale bars: 50 μm.

(Fig. 6A, right panel). In the absence of inhibitor (–Y), the differences in cell shape between controls and ILK-deficient cells are striking, whereas inhibition of Rho–ROCK signaling by Y-27632 (+Y) induced formation of large lamellipods in some cells.

These results suggest that ILK-deficient fibroblasts exhibit enhanced Rho–ROCK activity. These cells should therefore display higher levels of the ROCK-mediated phosphorylated form of MLC (MLC-*P*) (Huveneers and Danen, 2009). This was indeed confirmed by western blot analysis, which revealed significantly higher MLC-*P* levels in ILK-deficient cells compared with control cells ($P<0.05$; $n=4$) (Fig. 6C). Treatment with Y-27632 abrogated MLC phosphorylation in both genotypes. As these results provided indirect evidence for enhanced RhoA activity, we used G-linked immunosorbent assay (G-LISA) to directly confirm elevated RhoA activity in ILK-deficient fibroblasts (Fig. 6D).

Impaired directional migration and activation of Rac1 in ILK-deficient fibroblasts

The failure of ILK-deficient fibroblasts to spread properly could also be due to reduced Rac1 activity. Levels of GTP-loaded Rac1

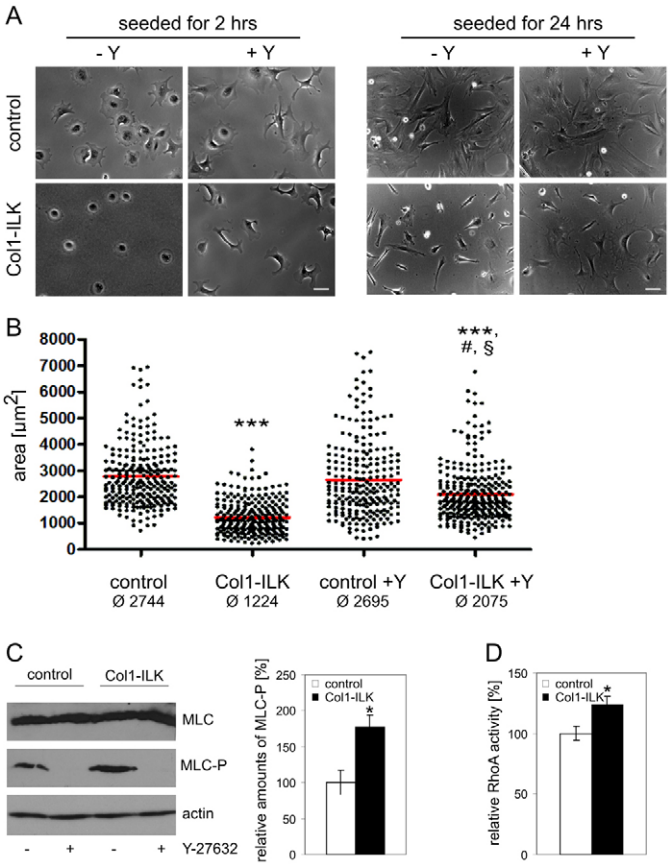

Fig. 6. Partial rescue of abnormal cell morphology by inhibition of Rho–ROCK signaling. Phase-contrast images of ILK-deficient and control fibroblasts, starved overnight in 1% FCS, then reseeded onto glass surfaces coated with 10 ng/ml fibronectin in the absence or presence of 5 µM Y-27632 (ROCK inhibitor) for 2 hours (**A**, left panels). In addition, cells were also starved overnight, reseeded onto tissue culture plastic and cultured for 24 hours before incubation with Y-27632 for 2 hours (A, right panels). Scale bars: 50 µm. (**B**) Quantification of the area covered by ILK-deficient and control fibroblasts shown in the left panels of A. Each dot represents one cell; n>224 per genotype and condition. ***difference to control; $^{\#}$difference to Col1-ILK; §difference to control + Y; all differences are highly significant (P<0.0001). (**C**) Protein extracts from starved ILK-deficient and control fibroblasts, grown for 12 hours on tissue-culture plastic and incubated with Y-27632 for 2 hours, were probed for amounts of MLC and phosphorylated MLC (MLC-P). Quantification revealed significantly increased levels of MLC-P in ILK-deficient fibroblasts (P<0.05). (**D**) Elevated levels of active RhoA were assessed by G-LISA in lysates from serum-starved control and ILK-deficient fibroblasts after 5 minutes of serum stimulation (n=4; P=0.002). Error bars are ± s.d.

were therefore assessed in control and ILK-deficient fibroblasts by pull-down assays with serum-starved fibroblasts. Levels of active Rac1 were strongly reduced in ILK-deficient fibroblasts in comparison to controls (Fig. 7A). Because Rac1 activity is also required for the extension and stabilization of lamellipodia at the leading edge of migrating cells (Ridley, 2000), and reduced migration could contribute to the paucity of cells observed in the granulation tissue of Col1-ILK mice, we analyzed migration of growth-arrested cells into scratch wounds by assessing the size of the free space that was not covered by migrating cells. Whereas control cells repopulated the free area within 10 hours, wounds in cultures of ILK-deficient fibroblasts were significantly larger

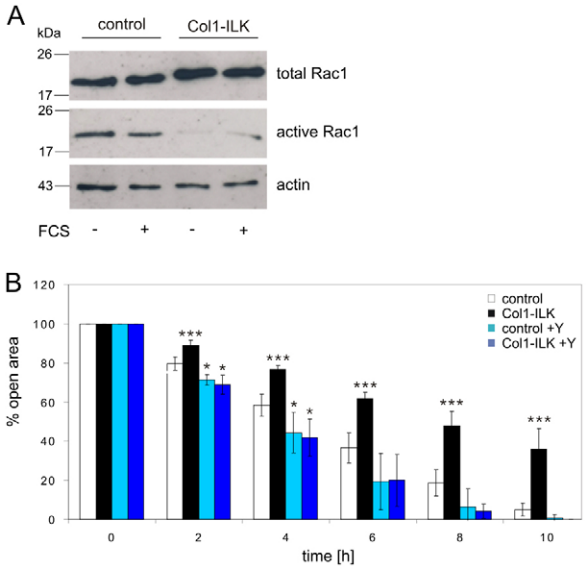

Fig. 7. Reduced activation of Rac1 and directional migration in ILK-deficient fibroblasts. (**A**) Levels of active Rac1 in ILK-deficient and control fibroblasts were assessed by pull-down using PAK-CRIB after starving the cells overnight and stimulating with 10% FCS for 45 minutes. The blot shows comparable levels of total Rac1 in ILK-deficient and control fibroblasts, whereas the fraction of active Rac1 was nearly undetectable in ILK-deficient cells. Representative of n=3 experiments. (**B**) Migration into scratch wounds of growth-arrested ILK-deficient fibroblasts (black bars) was significantly delayed over 10 hours in comparison with controls (white bars) (*P<0.05; ***P<0.0001; n=6). Addition of 5 µM Y-27632 enhanced migration – reflected by the reduced cell-free, open area – of control (light blue) and ILK-deficient (dark blue) fibroblasts to comparable values. Error bars are ± s.d.

beyond 10 hours (Fig. 7B, white and black bars; P<0.0001; n=6). Suppression of Rho–ROCK signaling by Y-27632 stimulated wound closure in cells of both genotypes, and abolished differences between ILK-deficient and control cells, inferring rescue of migration (Fig. 7B, blue bars).

Inhibition of RhoA–ROCK signaling restores TGFβ1 levels in ILK-deficient fibroblasts

Having established that ablation of ILK in fibroblasts leads to reduced extracellular TGFβ1 levels, which appear to be responsible for defective conversion of fibroblasts to myofibroblasts, as well as to increased RhoA–ROCK activity, which appears to determine cell shape and migratory capacity, the question arises as to whether these two effects are linked. We addressed this question by assessing levels of total TGFβ1 in supernatants of ILK-deficient and control fibroblasts cultured in stressed lattices in the absence (see also Fig. 3C) and presence of Y-27632. These experiments confirmed reduction of TGFβ1 levels to 46% of control levels in untreated ILK-deficient fibroblasts (Fig. 8). Inhibition of RhoA–ROCK signaling, however, resulted in a significant increase of TGFβ1 to 72% of control levels (P=0.018), which corresponds to the magnitude of rescue in cell area by Y-27632 (Fig. 6B).

We thus conclude that ablation of ILK in fibroblasts induces increased RhoA–ROCK activity and abnormal morphology, which result in decreased extracellular TGFβ1 activity and failure to produce sufficient αSMA for myofibroblast conversion. Concomitantly, Rac1 activity is reduced and cell migration is impaired.

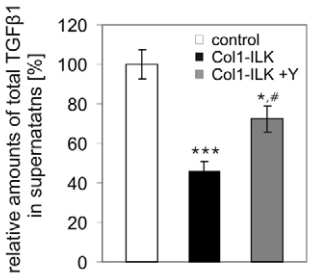

Fig. 8. Significant change in TGFβ1 produced by ILK-deficient fibroblasts following inhibition of RhoA–ROCK signaling. Control and ILK-deficient fibroblasts were cultured in tethered collagen lattices (see Fig. 3C) in 1% FCS without or with 5 μM Y-27632 for 24 hours. Amounts of total secreted TGFβ1 were assessed using mink lung epithelial cells, revealing a significant increase in TGFβ1 in supernatants of ILK-deficient lattice cultures after addition of Y-27632. ***P=0.0008 compared with control; *P=0.027 compared with control; $^{\#}P$=0.018 compared with Col1-ILK. Error bars are ± s.d.

Discussion

This study addressed the functional relevance of ILK for skin fibroblast functions in vivo and in vitro. Our results suggest that ILK is necessary to provide a structural link for matrix adhesion sites capable of bearing tensile force, to limit RhoA activity and to promote release of TGFβ1, and that it is an essential component of matrix adhesions for the differentiation of fibroblasts to myofibroblasts, their migration into wound sites and re-establishing a normal dermis.

In vivo analysis of ILK function in fibroblasts was achieved by breeding $Ilk^{fl/fl}$ mice with a strain that carries a tamoxifen-inducible Cre recombinase under the control of a minimal α2(I) procollagen promoter linked to a fibroblast-specific enhancer (Denton et al., 2009; Liu et al., 2009; Sonnylal et al., 2007; Zheng et al., 2002). Efficient deletion of ILK was seen in fibroblasts of Col1-ILK mice, but not in keratinocytes or endothelial cells.

To investigate the contribution of ILK to activation of fibroblasts during tissue repair, we explored granulation tissue formation in excisional wounds. Induced deletion of ILK in fibroblasts in mice did not affect the influx of inflammatory cells, formation of blood vessels or re-epithelialization. However, deletion resulted in perturbed formation of granulation tissue in healing wounds, characterized by virtual absence of myofibroblasts, strongly diminished deposition of dermal matrix and contraction of granulation tissue, and reduced dermal cell density.

To dissect fibroblast-autonomous defects aside from the complex tissue environment, primary fibroblasts were cultured from the dermis of tamoxifen-injected Col1-ILK and control mice. In comparison with controls, ILK-deficient fibroblasts were much smaller and characterized by a needle-like shape, reduced spreading, and disorganized actin cytoskeleton and matrix adhesions on substrates engaging β1 and β3 integrins. Reduced spreading was not due to reduced expression of integrin receptors and probably not to differences in integrin conformation and, hence, in ligand affinity and activation status (Banno and Ginsberg, 2008; Hughes and Pfaff, 1998). Normal surface expression levels of several integrin subunits including β1 integrin were also reported for keratinocytes, chondrocytes and vascular smooth muscle cells lacking ILK (Grashoff et al., 2003; Lorenz et al., 2007; Montanez et al., 2009).

The low cell density observed in wounds of Col1-ILK mice prompted the analysis of proliferative potential. Reduced numbers of Ki67-positive cells were detected in mutant wounds, indicating reduced proliferation of mutant cells. This is in contrast to our in vitro findings, which show that proliferation of *Ilk*-null fibroblasts in two- or three-dimensional cultures did not differ significantly from controls. This discrepancy may be explained by the complex wound environment, in which mutant fibroblasts might not be able to respond adequately to the different triggers. Impaired migration of ILK-deficient fibroblasts into the wound area might further add to an overall lower cell density within the wound.

Virtually all cell types rendered ILK-deficient, ranging from *Caenorhabditis elegans* (Norman et al., 2007), zebrafish (Postel et al., 2008), *Drosophila* (Zervas et al., 2001) to mice (Gheyara et al., 2007; Hannigan et al., 2007; Lorenz et al., 2007; Nakrieko et al., 2008; Sakai et al., 2003; this report), exhibit disruption of actin cytoarchitecture and matrix adhesions. In fibroblasts, these structures are prerequisites for fulfilling dynamic functions (Bershadsky et al., 2006; Goffin et al., 2006) and, accordingly, spreading, migration and matrix contraction by ILK-deficient fibroblasts were strongly impaired. In contrast to other cell types and specific to fibroblasts is the observed differentiation defect, which results in impaired formation of myofibroblasts. We conclude that generation of this specialized ECM-synthesizing, contractile, αSMA-positive fibroblast is precluded because matrix adhesions without ILK assemble into structurally abnormal complexes that fail to bear or transmit the required mechanical tension. The structural defect in ILK-deficient fibroblasts could be the absence of the link between ILK and PINCH, parvin and/or α-PIX similarly to that in contractile smooth muscle cells, in which ILK regulates neuronal Wiskott-Aldrich syndrome protein (N-WASP)-mediated actin polymerization, cell contraction and development of mechanical tension (Zhang et al., 2007). Kindlin-2 is another protein that binds directly to ILK in matrix adhesions of fibroblasts and also to integrin β1 tails, and cooperates with talin in integrin activation (Harburger et al., 2009; Larjava et al., 2008; Montanez et al., 2008). Kindlin-2 expression has been shown to be retained in ILK-deficient fibroblasts (Montanez et al., 2008), where it might provide some functional compensation for the loss of ILK.

Specific defects in mechanotransduction have also been reported in ILK-deficient fibroblast-like cells, which were not derived from the dermis of mouse skin, but from embryos (Maier et al., 2008). Upon mechanical loading in vitro, these cells failed to exhibit responses typical for mechanically stressed fibroblasts. By contrast, phosphorylation of ERK1 and/or ERK2, focal adhesion kinase and protein kinase B (PKB, also known as Akt) in response to stress was identical in ILK-deficient and control cells.

Besides mechanical tension, myofibroblast formation strictly requires TGFβ1, which is pivotal for fibroblast function in inflammation, scarring and fibrosis (Denton et al., 2009; Hinz, 2007; Tomasek et al., 2002). Synthesis of TGFβ1 itself is positively regulated by mechanical stress in fibroblasts at the transcriptional level (Kessler et al., 2001). Moreover, TGFβ1 can be activated from extracellular stores by mechanical deformation of LAP in an integrin-dependent mechanism (Wipff et al., 2007). Our results suggest that gene expression and the percentage of latent TGFβ1 conversion to its active form are not impaired in ILK-deficient fibroblasts in collagen lattices under stress. However, levels of extracellular active and total TGFβ1 in conditioned medium appeared to be coordinately regulated and were both strongly reduced in ILK-deficient fibroblasts. This strict correlation between

the amount of latent TGFβ1 available to the cells and the TGFβ1 activity generated has been observed previously, e.g. in fibroblast–keratinocyte co-cultures (Shephard et al., 2004), and is apparently not due to auto-induction of TGFβ synthesis. Thus, our data indicate that *Ilk*-null fibroblasts have a defect in TGFβ homeostasis, i.e. the cells are impaired in their capacity to maintain extracellular TGFβ1 levels. Regarding potential mechanisms explaining this defect, reduced transcription and RNA stability can be ruled out, as *Tgfb1* RNA steady-state levels are similar in control and *Ilk*-null fibroblasts, pointing to defects in post-transcriptional events. These could be related to decreased protein synthesis, altered intracellular modification, defective processing of pro-TGFβ (Yang et al., 2010) or altered assembly of the large latent complex, all of these potentially resulting in decreased latent TGFβ1 secretion and activation (Miyazono et al., 1991; Saharinen et al., 1996). Decreased secretion of factors including TGFβ1 has been reported for other cell types that lack ILK. TGFβ1 secretion was impaired in mesangial cells transfected with a kinase-dead mutant of ILK (Ortega-Velazquez et al., 2004). Inhibition of ILK by knockdown (Lin et al., 2007) or by small molecule inhibitors (Edwards et al., 2008) also resulted in selected suppression of secreted vascular endothelial growth factor and urokinase plasminogen activator levels, but not those of PAI-1, indicating that ILK is involved in specific intracellular protein processing events and/or secretory pathways. Alternatively, proteolytic mobilization of latent TGFβ1 from extracellular growth factor deposits, on the cell surface or in the ECM, might be impaired, leading to reduced levels of TGFβ1 precursor available to the cells for activation.

TGFβ receptors are functional in mutant fibroblasts, as was demonstrated by normal Smad signaling following addition of exogenous TGFβ1. This treatment was sufficient to rescue production of αSMA and its incorporation into stress fibers, confirming the strict dependence of this differentiation process on TGFβ1, and to largely rescue collagen lattice contraction. These data highlight the importance of TGFβ1 activity in the immediate vicinity of fibroblasts for myofibroblast formation. In healing wounds, TGFβ1 is thought to be supplied mainly by platelets and macrophages, particularly at early stages (Eming et al., 2007). Other cell types, such as fibroblasts, keratinocytes and vascular cells, probably contribute to latent TGFβ secretion and/or activation (Brunner and Blakytny, 2004), resulting in a second peak of TGFβ activity upon wound closure (Yang et al., 1999). Because the influx of inflammatory cells, as well as angiogenesis, were not altered in our system, it appears that the fibroblasts themselves are responsible for mobilizing and activating sufficiently high amounts of TGFβ1 in the immediate vicinity of fibroblasts and that this is crucial to ensure myofibroblast differentiation. This is further supported by the observation that keratinocyte proliferation is reduced rather than increased. Since TGFβ1 is a potent negative regulator of epithelial growth (Massague, 2000; Shipley et al., 1986), this observation suggests that reduced release of TGFβ1 by mutant fibroblasts is a local phenomenon that is restricted to the immediate fibroblast environment, and does not result in generally lower TGFβ1 concentrations in the healing wound.

Addition of exogenous TGFβ1 clearly did not change the small size, lack of spreading and overall fibroblast morphology that was caused by inactivation of ILK. Concomitant with low Rac1 activity, we found increased RhoA–ROCK activity and enhanced phosphorylation of MLC in ILK-deficient fibroblasts, which was inhibited by Y-27632. Suppression of RhoA–ROCK signaling enabled almost normal cell spreading and migration. The inhibitory effects by Y-27632 on levels of MLC-*P*, cell morphology and migration, as well as TGFβ levels, were extensive, whereas an increase in RhoA activity in ILK-deficient fibroblasts was surprisingly less pronounced. An explanation for this might be that Y-27632 also modulates the activity of other kinases beyond ROCK, such as PKCε (Ishizaki et al., 2000; Uehata et al., 1997). Although the affinity of Y-27632 is markedly higher for Rho-associated kinases, other kinases could potentially also contribute to the observed defects in ILK-deficient fibroblasts.

The observation of delayed collagen lattice contraction by ILK-deficient cells is in agreement with our previous work, which reported delayed collagen lattice reorganization and contraction by fibroblasts expressing constitutively active RhoA (Zhang et al., 2006b), and can be explained by the concept that lattice reorganization by fibroblasts is mediated by cell migration and traction (Harris et al., 1981).

We conclude that, in fibroblasts, ILK functions as a negative regulator of RhoA activity (Montanez et al., 2009). The exact mechanism by which ILK controls RhoA signaling remains elusive. Interestingly, a recent report indicates that the ILK–α-parvin complex is involved in limiting RhoA activity. Thus, ablation of α-parvin in vascular smooth muscle cells resulted in a similar phenotype to the one described here, with similarly elevated RhoA levels and spreading defects. The phenotype is more severe in fibroblasts, probably because the ILK–α-parvin complex cannot assemble (Legate et al., 2006), whereas in the mural cells used by Montanez and colleagues, an independent ILK–β-parvin complex forms and compensates, to some extent, for the absence of α-parvin (Montanez et al., 2009). Mechanistically, high RhoA activity might be achieved by lack of direct inhibitory action of Rac1 on RhoA, or, indirectly, by low amounts or activity of Rho GTPase activating proteins, which normally limit amounts of the active, GTP-bound form of Rho. Increased RhoA–ROCK activity was further reported in cells with defective spreading and migration following transfection with EphA1, a tyrosine kinase receptor for ephrin-A. Interestingly, ILK was downregulated in these cells (Yamazaki et al., 2009).

Our current results do not allow to us conclude whether ablation of ILK in fibroblasts first results in increased RhoA–ROCK activity, which then stimulates decreased Rac1 activity, or vice versa. However, they show that TGFβ1 production by fibroblasts is under the control of Rho activity, possibly by regulating post-transcriptional events involved in processing, assembling, secreting or mobilizing the large latent TGFβ complex. In summary, this study reveals the central function of ILK in the generation of myofibroblasts by two mechanisms. First, it serves as a structural adaptor, orchestrating the proper topology of integrin-containing matrix adhesions, which are required for efficient mechanotransduction. Second, ILK controls fibroblast morphology and migration by limiting Rho–ROCK signaling, which, in turn, regulates TGFβ1 production required for myofibroblast conversion and mechanical tension. Impairment of these functions explains the insufficient myofibroblast differentiation and migration into granulation tissue, which compromises dermal wound healing in mice with fibroblast-restricted deletion of ILK, but might be beneficial in protection from fibrosis. Although the effects are most pronounced in fibroblasts, these mechanisms are not restricted to these cells and, in fact, appear to operate in several cell types (Montanez et al., 2009) and might thus be of general biological significance.

Materials and Methods

Generation of mice with inducible fibroblast-specific ILK ablation

Mice with a floxed exon 2 containing the translation start ATG (Grashoff et al., 2003; Sakai et al., 2003) were bred to a mouse line that expresses inducible Cre recombinase under the control of a fibroblast-specific regulatory fragment of the pro-α2(I) collagen gene (*Col1a2*) (Zheng et al., 2002). Genotyping was performed using PCR for the presence of the floxed (370 bp) or wild-type (296 bp) *Ilk* allele (forward primer 5′-GTCTTGCAAACCCGTCTCTGCG-3′; reverse primer 5′-CAGAGGTGTC-AGTGCTGGGATG-3′) and for *Cre* (forward primer 5′-GACGGAAATCCA-TCGCTCGA-3′; reverse primer 5′-GACATGTTCAGGGATCGCCA-3′). Cre activity was initiated by intraperitoneal injection of 1 mg of tamoxifen (20 mg/ml stock in sunflower seed oil; Sigma) per mouse per day on five consecutive days into 12-day-old mice. Animals were housed in specific pathogen-free facilities. All animal protocols were approved by the local veterinary authorities.

Wounding and tissue harvesting

Female animals that carried the *Cre* gene and were homozygous for the Ilk^{fl} allele (Col1-ILK) were used as experimental animals at ~3 weeks of age (2–5 days after the last tamoxifen injection). Females that were either $Ilk^{fl/+}$; *Cre*-positive or *Cre*-negative were used as controls. All animals were derived as offspring from matings between $Ilk^{fl/+}$; *Cre*-positive and $Ilk^{fl/+}$; *Cre*-negative animals on a mixed background. On the shaved backs, one full-thickness wound, comprising the skin and subcutaneous panniculus carnosus muscle, of 4 mm in diameter was inflicted on each side of the scapular region using biopsy punches under isoflurane anesthesia and left uncovered to heal.

Histology, immunohistochemistry and immunofluorescence analysis

Wounds were bisected and either frozen unfixed in optimal cutting temperature (OCT) compound (Sakura) or fixed for 3 hours in 4% paraformaldehyde solution before paraffin embedding. Cryosections of 6 μm were mounted on polylysine-coated slides and fixed for 30 minutes in ice-cold methanol. For general histology, paraffin-embedded sections were stained with hematoxylin and eosin (H&E) or Masson's trichrome following standard procedures. Cell proliferation was assessed by immunohistochemistry using antibodies against Ki67 (TEC-3, Dako), followed by biotin-conjugated secondary antibodies. For immunofluorescence, sections were blocked with the appropriate normal serum (Dako) before application of primary antibodies. Cells were permeabilized (0.2% Triton X-100 in PBS, 10 minutes at room temperature) before blocking. Primary antibodies were as follows: αSMA (Cy3-conjugated clone 1A4, Sigma), ILK (I-1907, Sigma), phalloidin–Alexa-Fluor-594 (Molecular Probes, Invitrogen) and vinculin (MAB 3574, Chemicon, Millipore). Secondary antibodies were coupled to Alexa Fluor 488 or Alexa Fluor 594 (Molecular Probes, Invitrogen). Nuclei were counterstained either with propidium iodide or DAPI. Photomicrographs were taken using either a DM 4000B microscope (Leica) or a Nikon Eclipse 800E fluorescence microscope equipped with a digital camera (DXM 1200F; Nikon). Image analysis was performed using Lucia software (Laboratory Imaging) or DISKUS (Hilgers).

Isolation, culture and characterization of primary fibroblasts

Fibroblasts were cultured from the dermis of 3-week-old animals as previously described (Zweers et al., 2007) after tamoxifen induction and genotyping, and were used between passages 1 and 6. Briefly, trunk skin was minced and digested with 400 units/ml of collagenase I (Cell Systems) for 2 hours at 37°C. The homogenate was cleared by passing through a cell sieve (Falcon), and cells were cultured in DMEM (Invitrogen) containing 10% FCS (Thermo Scientific), 50 μg/ml Na-ascorbate (Sigma), 2 mM glutamine and antibiotics (Seromed-Biochrom) at 37°C in 5% CO_2 on tissue-culture plastic (Becton Dickinson Labware). Because prolonged culture of incompletely deleted fibroblast populations can result in overgrowth of undeleted cells, genotypes were routinely confirmed in all experiments. For immunofluorescence, cells were seeded on Permanox chamberslides or on chambers with glass bottoms (Nunc, Thermo Scientific) that were coated with bovine collagen I (30 μg/ml in PBS; IBFB, Curacyte) or human fibronectin (10 μg/ml; Sigma). TGFβ1 (recombinant human, R&D Systems) was added to serum-deprived cultures at a concentration of 10 ng/ml in DMEM with 1% FCS directly at culture onset for 24 hours. ROCK inhibitor Y-27632 (Calbiochem) was added at 5 μM as specified.

Collagen lattice culture

Fibroblasts were starved overnight in DMEM with 1% FCS, ascorbate, antibiotics and glutamine, and then seeded in the same medium at 7×10^4 cells per gel (500 μl) into 24-well plates with 0.3 mg/ml of acid-extracted collagen I from newborn calf skin (IBFB, Curacyte) as previously described (Kessler et al., 2001; Zhang et al., 2006a). Lattices were detached manually to facilitate contraction. Tethered lattices were cast with 2×10^5 fibroblasts per lattice (6 ml), as described above, into 6 cm dishes. Braided nylon rings inserted into the dishes kept the lattices from shrinking (Kessler et al., 2001). For western blot analysis, fibroblasts were liberated from the lattices by incubation with 400 U/ml collagenase I (Cell Systems) in serum-free DMEM for 15 minutes at 37°C.

Cell migration analysis in vitro

Fibroblasts were growth-arrested by mitomycin C treatment (Sigma; 4 μg/ml for 2 hours at 37°C) and seeded at high density (50,000 cells/cm^2) in DMEM with 1% FCS. Scratch wounds of ~1 mm width were introduced with a disposable pipette tip. Cell migration into the denuded area was monitored for 10 hours in the absence or presence of 5 μM Y-27632 in an incubator chamber attached to an IX81 microscope (Olympus) at 37°C, 5% CO_2 and 60% humidity. Frames were taken every 30 minutes using an OBS CCD FV2T camera, and the extent of remaining free area was quantified using OBS Cell R software (Olympus).

TGFβ1 activity bioassay

TGFβ1 levels were assessed in 24-hour conditioned medium of tethered collagen lattice cultures that were cast in DMEM with 1% FCS with or without 5 μM Y-27632. TGFβ activity was determined in the plasminogen activator inhibitor-1 (PAI-1)/luciferase (PAI/L) assay (Abe et al., 1994) using mink lung epithelial cells stably transfected with a luciferase reporter gene under the control of a TGFBβ-specific, truncated PAI-1 promoter (a gift from Daniel B. Rifkin, New York University Medical Center, New York, NY). Samples were assayed at two dilutions to fit into the linear range of the assay (5–250 pg/ml). Total TGFβ activity was determined following heat activation of the samples for 10 minutes at 80°C. Following overnight incubation of the reporter cells with the samples or with recombinant human TGFβ1 standards, cells were lysed and luciferase activity determined using an MLX Microtiter Plate Luminometer (Dynex Technologies).

Rac and RhoA activity assays

Rac activity was assayed with a biotinylated peptide corresponding to the CRIB motif of the Rac1 effector Pak, essentially as described previously (Price et al., 2003). Confluent fibroblast cultures were starved overnight in medium without FCS and activated by addition of 10% FCS for 45 minutes. Cells were washed with PBS and scraped off the plates into 700 μl lysis buffer (50 mM Tris-HCl pH 7.4, 100 mM NaCl, 10 mM $MgCl_2$, 1% NP-40 and protease inhibitor mix; Sigma). Three μl of the CRIB peptide (2 mg/ml; Biotrend) were added, and lysates were rotated for 45 minutes at 4°C. After clearing by centrifugation, an aliquot of total lysates was removed and remaining lysates were rotated another 45 minutes at 4°C. The latter were then incubated with 30 μl streptavidin-agarose beads (Novagen, Merck) for 30 minutes at 4°C. The beads were washed, and bead samples and equal amounts of total lysate were separated by SDS-PAGE. Rac was detected by western blotting using an anti-Rac1 antibody (clone 23A4; Upstate Biotechnology, Millipore). RhoA activity was assessed using G-LISA (#BK124, Cytoskeleton) according to the manufacturer's protocol. Serum-starved cells were reseeded at 400,000 cells per 6 cm culture dish for 6 hours, stimulated for 5 minutes with FCS and lysates were snap-frozen in liquid nitrogen prior to applying to G-LISA assay.

RT-PCR, northern and western immunoblot analysis

Northern blot hybridization was carried out as previously described (Kessler et al., 2001) using ^{32}P-labeled probes. The TGFβ1 cDNA probe was generated by reverse transcription of total wild-type mouse RNA (Fermentas) and PCR amplification of a 300 bp fragment of murine TGFβ1 (forward primer 5′-CAACGCCAT-CTATGAGAAAACC-3′; reverse primer 5′-AAGCCCTGTATTCCGTCTCC-3′). Hybridization with a probe detecting 18S rRNA was used to control for equal loading as previously described (Kessler et al., 2001). TGFβ1 transcript levels were also assessed by semi-quantitative RT-PCR using forward 5′-CAACGCC-ATCTATGAGAAAACC-3′ and reverse 5′-AAGCCCTGTATTCCGTCTCC-3′ primers to amplify a 300 bp product of TGFβ1 cDNA (Fermentas) and forward 5′-AATGTGCAGCCCATTCGCTG-3′ and reverse 5′-CTTCCGTCCTTACAA-AACGG-3′ primers for the product (324 bp) of S26 cDNA, which was used for normalization.

Proteins for western blot analyses were extracted in RIPA buffer (150 mM NaCl, 50 mM Tris-HCl, 1% NP-40, 0.1% SDS, 0.5% Na-deoxycholate, 5 mM EDTA, 1% Triton X-100, pH 8), supplemented with protease and phosphatase inhibitor cocktails (Sigma), separated by SDS-PAGE and transferred to Hybond C extra membranes (Amersham Biosciences). Fibroblasts in tethered collagen lattices were first liberated by digestion with collagenase (400 U/ml CLS1, for 15 minutes at 37°C in serum-free DMEM; Cell Systems) before lysis in RIPA buffer. Following blocking (5% milk powder in TBS-T, pH 7.6), membranes were incubated with primary antibodies in blocking solution. Signals were detected by chemiluminescence using Western Lightning (Perkin Elmer) or SuperSignal West Femto (Thermo Scientific). Primary antibodies used were directed against αSMA (clone 1A4, Sigma), ILK (I-1907, Sigma), phosphorylated Smad2 (recognizing Ser465 and Ser467; Cell Signaling/New England Biolabs #3101), MLC (clone MY-21, Sigma), phosphorylated MLC (#3674, Cell Signaling) and actin (MP Biomedicals). Secondary HRP-conjugated antibodies were purchased from Dako. Identical gels run in parallel and stained with Coomassie Blue were used as loading control. Signals were quantified by densitometry using ImageJ (http://rsbweb.nih.gov/ij).

Statistical evaluation

Results are presented as means ± s.d. Statistical analysis was performed using unpaired Student's *t*-tests, and $P<0.05$ was considered statistically significant. Calculations were performed using GraphPad Prism (GraphPad Software)

We thank Roswitha Nischt, Paola Zigrino, Zhigang Zhang, Monique Aumailley, Sabine Eming and Carien Niessen (Cologne) for insightful discussion; Gabi Scherr, Nicole Pohl, Ute Hillebrand (Cologne) and Tamara Berger (Münster) for excellent technical assistance; Carien Niessen for the generous gift of PAK-CRIB peptide; and Kristina Behrendt (Cologne) for help with the Rac pull-down. This work was supported by Deutsche Forschungsgemeinschaft through EC140/5-1 and SFB 829 (to B.E. and T.K.).

Supplementary material available online at
http://jcs.biologists.org/cgi/content/full/123/??/????/DC1

References

Abe, M., Harpel, J. G., Metz, C. N., Nunes, I., Loskutoff, D. J. and Rifkin, D. B. (1994). An assay for transforming growth factor-beta using cells transfected with a plasminogen activator inhibitor-1 promoter-luciferase construct. *Anal. Biochem.* **216**, 276-284.

Aluwihare, P., Mu, Z., Zhao, Z., Yu, D., Weinreb, P. H., Horan, G. S., Violette, S. M. and Munger, J. S. (2009). Mice that lack activity of alphavbeta6- and alphavbeta8-integrins reproduce the abnormalities of Tgfb1- and Tgfb3-null mice. *J. Cell Sci.* **122**, 227-232.

Annes, J. P., Chen, Y., Munger, J. S. and Rifkin, D. B. (2004). Integrin alphaVbeta6-mediated activation of latent TGF-beta requires the latent TGF-beta binding protein-1. *J. Cell Biol.* **165**, 723-734.

Banno, A. and Ginsberg, M. H. (2008). Integrin activation. *Biochem. Soc. Trans.* **36**, 229-234.

Bershadsky, A. D., Ballestrem, C., Carramusa, L., Zilberman, Y., Gilquin, B., Khochbin, S., Alexandrova, A. Y., Verkhovsky, A. B., Shemesh, T. and Kozlov, M. M. (2006). Assembly and mechanosensory function of focal adhesions: experiments and models. *Eur. J. Cell Biol.* **85**, 165-173.

Brunner, G. and Blakytny, R. (2004). Extracellular regulation of TGF-beta activity in wound repair: growth factor latency as a sensor mechanism for injury. *Thromb. Haemost.* **92**, 253-261.

Chrzanowska-Wodnicka, M. and Burridge, K. (1996). Rho-stimulated contractility drives the formation of stress fibers and focal adhesions. *J. Cell Biol.* **133**, 1403-1415.

Crawford, S. E., Stellmach, V., Murphy-Ullrich, J. E., Ribeiro, S. M., Lawler, J., Hynes, R. O., Boivin, G. P. and Bouck, N. (1998). Thrombospondin-1 is a major activator of TGF-beta1 in vivo. *Cell* **93**, 1159-1170.

Cukierman, E., Pankov, R. and Yamada, K. M. (2002). Cell interactions with three-dimensional matrices. *Curr. Opin. Cell Biol.* **14**, 633-639.

Denton, C. P., Khan, K., Hoyles, R. K., Shiwen, X., Leoni, P., Chen, Y., Eastwood, M. and Abraham, D. J. (2009). Inducible lineage-specific deletion of TbetaRII in fibroblasts defines a pivotal regulatory role during adult skin wound healing. *J. Invest. Dermatol.* **129**, 194-204.

Desmouliere, A., Chaponnier, C. and Gabbiani, G. (2005). Tissue repair, contraction, and the myofibroblast. *Wound Repair. Regen.* **13**, 7-12.

Edwards, L. A., Woo, J., Huxham, L. A., Verreault, M., Dragowska, W. H., Chiu, G., Rajput, A., Kyle, A. H., Kalra, J., Yapp, D. et al. (2008). Suppression of VEGF secretion and changes in glioblastoma multiforme microenvironment by inhibition of integrin-linked kinase (ILK). *Mol. Cancer Ther.* **7**, 59-70.

Eming, S. A., Krieg, T. and Davidson, J. M. (2007). Inflammation in wound repair: molecular and cellular mechanisms. *J. Invest. Dermatol.* **127**, 514-525.

Gabbiani, G. (2003). The myofibroblast in wound healing and fibrocontractive diseases. *J. Pathol.* **200**, 500-503.

Gheyara, A. L., Vallejo-Illarramendi, A., Zang, K., Mei, L., St-Arnaud, R., Dedhar, S. and Reichardt, L. F. (2007). Deletion of integrin-linked kinase from skeletal muscles of mice resembles muscular dystrophy due to alpha 7 beta 1-integrin deficiency. *Am. J. Pathol.* **171**, 1966-1977.

Goffin, J. M., Pittet, P., Csucs, G., Lussi, J. W., Meister, J. J. and Hinz, B. (2006). Focal adhesion size controls tension-dependent recruitment of alpha-smooth muscle actin to stress fibers. *J. Cell Biol.* **172**, 259-268.

Grashoff, C., Aszodi, A., Sakai, T., Hunziker, E. B. and Fassler, R. (2003). Integrin-linked kinase regulates chondrocyte shape and proliferation. *EMBO Rep.* **4**, 432-438.

Grinnell, F. (2003). Fibroblast biology in three-dimensional collagen matrices. *Trends Cell. Biol.* **13**, 264-269.

Hannigan, G. E., Leung-Hagesteijn, C., Fitz-Gibbon, L., Coppolino, M. G., Radeva, G., Filmus, J., Bell, J. C. and Dedhar, S. (1996). Regulation of cell adhesion and anchorage-dependent growth by a new beta 1-integrin-linked protein kinase. *Nature* **379**, 91-96.

Hannigan, G. E., Coles, J. G. and Dedhar, S. (2007). Integrin-linked kinase at the heart of cardiac contractility, repair, and disease. *Circ. Res.* **100**, 1408-1414.

Harburger, D. S., Bouaouina, M. and Calderwood, D. A. (2009). Kindlin-1 and -2 directly bind the C-terminal region of beta integrin cytoplasmic tails and exert integrin-specific activation effects. *J. Biol. Chem.* **284**, 11485-11497.

Harris, A. K., Stopak, D. and Wild, P. (1981). Fibroblast traction as a mechanism for collagen morphogenesis. *Nature* **290**, 249-251.

Hinz, B. (2006). Masters and servants of the force: the role of matrix adhesions in myofibroblast force perception and transmission. *Eur. J. Cell Biol.* **85**, 175-181.

Hinz, B. (2007). Formation and function of the myofibroblast during tissue repair. *J. Invest. Dermatol.* **127**, 526-537.

Hinz, B., Mastrangelo, D., Iselin, C. E., Chaponnier, C. and Gabbiani, G. (2001). Mechanical tension controls granulation tissue contractile activity and myofibroblast differentiation. *Am. J. Pathol.* **159**, 1009-1020.

Hughes, P. E. and Pfaff, M. (1998). Integrin affinity modulation. *Trends Cell. Biol.* **8**, 359-364.

Humphries, M. J., Travis, M. A., Clark, K. and Mould, A. P. (2004). Mechanisms of integration of cells and extracellular matrices by integrins. *Biochem. Soc. Trans.* **32**, 822-825.

Huveneers, S. and Danen, E. H. (2009). Adhesion signaling-crosstalk between integrins, Src and Rho. *J. Cell Sci.* **122**, 1059-1069.

Hynes, R. O. (2002). Integrins: bidirectional, allosteric signaling machines. *Cell* **110**, 673-687.

Ishizaki, T., Uehata, M., Tamechika, I., Keel, J., Nonomura, K., Maekawa, M. and Narumiya, S. (2000). Pharmacological properties of Y-27632, a specific inhibitor of rho-associated kinases. *Mol. Pharmacol.* **57**, 976-983.

Kessler, D., Dethlefsen, S., Haase, I., Plomann, M., Hirche, F., Krieg, T. and Eckes, B. (2001). Fibroblasts in mechanically stressed collagen lattices assume a "synthetic" phenotype. *J. Biol. Chem.* **276**, 36575-36585.

Larjava, H., Plow, E. F. and Wu, C. (2008). Kindlins: essential regulators of integrin signalling and cell-matrix adhesion. *EMBO Rep.* **9**, 1203-1208.

Larsen, M., Artym, V. V., Green, J. A. and Yamada, K. M. (2006). The matrix reorganized: extracellular matrix remodeling and integrin signaling. *Curr. Opin. Cell Biol.* **18**, 463-471.

Legate, K. R., Montanez, E., Kudlacek, O. and Fassler, R. (2006). ILK, PINCH and parvin: the tIPP of integrin signalling. *Nat. Rev. Mol. Cell Biol.* **7**, 20-31.

Lin, S. W., Ke, F. C., Hsiao, P. W., Lee, P. P., Lee, M. T. and Hwang, J. J. (2007). Critical involvement of ILK in TGFbeta1-stimulated invasion/migration of human ovarian cancer cells is associated with urokinase plasminogen activator system. *Exp. Cell Res.* **313**, 602-613.

Liu, S., Kapoor, M. and Leask, A. (2009). Rac1 expression by fibroblasts is required for tissue repair in vivo. *Am. J. Pathol.* **174**, 1847-1856.

Lorenz, K., Grashoff, C., Torka, R., Sakai, T., Langbein, L., Bloch, W., Aumailley, M. and Fassler, R. (2007). Integrin-linked kinase is required for epidermal and hair follicle morphogenesis. *J. Cell Biol.* **177**, 501-513.

Maier, S., Lutz, R., Gelman, L., Sarasa-Renedo, A., Schenk, S., Grashoff, C. and Chiquet, M. (2008). Tenascin-C induction by cyclic strain requires integrin-linked kinase. *Biochim. Biophys. Acta* **1783**, 1150-1162.

Massague, J. (2000). How cells read TGF-beta signals. *Nat. Rev. Mol. Cell Biol.* **1**, 169-178.

Miyazono, K., Olofsson, A., Colosetti, P. and Heldin, C. H. (1991). A role of the latent TGF-beta 1-binding protein in the assembly and secretion of TGF-beta 1. *EMBO J.* **10**, 1091-1101.

Montanez, E., Ussar, S., Schifferer, M., Bosl, M., Zent, R., Moser, M. and Fassler, R. (2008). Kindlin-2 controls bidirectional signaling of integrins. *Genes Dev.* **22**, 1325-1330.

Montanez, E., Wickstrom, S. A., Altstätter, J., Chu, H. and Fässler, R. (2009). alpha-parvin controls vascular mural cell recruitment to vessel wall by regulating RhoA/ROCK signalling. *EMBO J.* **28**, 3132-3144.

Mu, D., Cambier, S., Fjellbirkeland, L., Baron, J. L., Munger, J. S., Kawakatsu, H., Sheppard, D., Broaddus, V. C. and Nishimura, S. L. (2002). The integrin alpha(v)beta8 mediates epithelial homeostasis through MT1-MMP-dependent activation of TGF-beta1. *J. Cell Biol.* **157**, 493-507.

Munger, J. S., Huang, X., Kawakatsu, H., Griffiths, M. J., Dalton, S. L., Wu, J., Pittet, J. F., Kaminski, N., Garat, C., Matthay, M. A. et al. (1999). The integrin alpha v beta 6 binds and activates latent TGF beta **1**, a mechanism for regulating pulmonary inflammation and fibrosis. *Cell* **96**, 319-328.

Murphy-Ullrich, J. E. and Poczatek, M. (2000). Activation of latent TGF-beta by thrombospondin-1: mechanisms and physiology. *Cytokine Growth Factor Rev.* **11**, 59-69.

Nakrieko, K. A., Welch, I., Dupuis, H., Bryce, D., Pajak, A., St Arnaud, R., Dedhar, S., D'Souza, S. J. and Dagnino, L. (2008). Impaired hair follicle morphogenesis and polarized keratinocyte movement upon conditional inactivation of integrin-linked kinase in the epidermis. *Mol. Biol. Cell* **19**, 1462-1473.

Nikolopoulos, S. N. and Turner, C. E. (2001). Integrin-linked kinase (ILK) binding to paxillin LD1 motif regulates ILK localization to focal adhesions. *J. Biol. Chem.* **276**, 23499-23505.

Nobes, C. D. and Hall, A. (1999). Rho GTPases control polarity, protrusion, and adhesion during cell movement. *J. Cell Biol.* **144**, 1235-1244.

Norman, K. R., Cordes, S., Qadota, H., Rahmani, P. and Moerman, D. G. (2007). UNC-97/PINCH is involved in the assembly of integrin cell adhesion complexes in Caenorhabditis elegans body wall muscle. *Dev. Biol.* **309**, 45-55.

Ortega-Velazquez, R., Gonzalez-Rubio, M., Ruiz-Torres, M. P., Diez-Marques, M. L., Iglesias, M. C., Rodriguez-Puyol, M. and Rodriguez-Puyol, D. (2004). Collagen I upregulates extracellular matrix gene expression and secretion of TGF-beta 1 by cultured human mesangial cells. *Am. J. Physiol. Cell Physiol.* **286**, C1335-C1343.

Popova, S. N., Barczyk, M., Tiger, C. F., Beertsen, W., Zigrino, P., Aszodi, A., Miosge, N., Forsberg, E. and Gullberg, D. (2007). Alpha11 beta1 integrin-dependent regulation of periodontal ligament function in the erupting mouse incisor. *Mol. Cell. Biol.* **27**, 4306-4316.

Postel, R., Vakeel, P., Topczewski, J., Knoll, R. and Bakkers, J. (2008). Zebrafish integrin-linked kinase is required in skeletal muscles for strengthening the integrin-ECM adhesion complex. *Dev. Biol.* **318**, 92-101.

Price, L. S., Langeslag, M., ten Klooster, J. P., Hordijk, P. L., Jalink, K. and Collard, J. G. (2003). Calcium signaling regulates translocation and activation of Rac. *J. Biol. Chem.* **278**, 39413-39421.

Ridley, A. (2000). Rho GTPases. Integrating integrin signaling. *J. Cell Biol.* **150**, F107-F109.

Rosenberger, G., Jantke, I., Gal, A. and Kutsche, K. (2003). Interaction of alphaPIX (ARHGEF6) with beta-parvin (PARVB) suggests an involvement of alphaPIX in integrin-mediated signaling. *Hum. Mol. Genet.* **12**, 155-167.

Saharinen, J., Taipale, J. and Keski-Oja, J. (1996). Association of the small latent transforming growth factor-beta with an eight cysteine repeat of its binding protein LTBP-1. *EMBO J.* **15**, 245-253.

Sakai, T., Li, S., Docheva, D., Grashoff, C., Sakai, K., Kostka, G., Braun, A., Pfeifer, A., Yurchenco, P. D. and Fassler, R. (2003). Integrin-linked kinase (ILK) is required for polarizing the epiblast, cell adhesion, and controlling actin accumulation. *Genes Dev.* **17**, 926-940.

Sander, E. E., ten Klooster, J. P., van Delft, S., van der Kammen, R. A. and Collard, J. G. (1999). Rac downregulates Rho activity: reciprocal balance between both GTPases determines cellular morphology and migratory behavior. *J. Cell Biol.* **147**, 1009-1022.

Sawada, Y. and Sheetz, M. P. (2002). Force transduction by Triton cytoskeletons. *J. Cell Biol.* **156**, 609-615.

Shephard, P., Martin, G., Smola-Hess, S., Brunner, G., Krieg, T. and Smola, H. (2004). Myofibroblast differentiation is induced in keratinocyte-fibroblast co-cultures and is antagonistically regulated by endogenous transforming growth factor-beta and interleukin-1. *Am. J. Pathol.* **164**, 2055-2066.

Sheppard, D. (2005). Integrin-mediated activation of latent transforming growth factor beta. *Cancer Metastasis Rev.* **24**, 395-402.

Sheppard, D. (2006). Transforming growth factor beta: a central modulator of pulmonary and airway inflammation and fibrosis. *Proc. Am. Thorac. Soc.* **3**, 413-417.

Shipley, G. D., Pittelkow, M. R., Wille, J. J., Jr, Scott, R. E. and Moses, H. L. (1986). Reversible inhibition of normal human prokeratinocyte proliferation by type beta transforming growth factor-growth inhibitor in serum-free medium. *Cancer Res.* **46**, 2068-2071.

Sonnylal, S., Denton, C. P., Zheng, B., Keene, D. R., He, R., Adams, H. P., Vanpelt, C. S., Geng, Y. J., Deng, J. M., Behringer, R. R. et al. (2007). Postnatal induction of transforming growth factor beta signaling in fibroblasts of mice recapitulates clinical, histologic, and biochemical features of scleroderma. *Arthritis Rheum.* **56**, 334-344.

Soriano, P. (1999). Generalized lacZ expression with the ROSA26 Cre reporter strain. *Nat. Genet.* **21**, 70-71.

Thannickal, V. J., Lee, D. Y., White, E. S., Cui, Z., Larios, J. M., Chacon, R., Horowitz, J. C., Day, R. M. and Thomas, P. E. (2003). Myofibroblast differentiation by transforming growth factor-beta1 is dependent on cell adhesion and integrin signaling via focal adhesion kinase. *J. Biol. Chem.* **278**, 12384-12389.

Tomasek, J. J., Gabbiani, G., Hinz, B., Chaponnier, C. and Brown, R. A. (2002). Myofibroblasts and mechano-regulation of connective tissue remodelling. *Nat. Rev. Mol. Cell Biol.* **3**, 349-363.

Tu, Y., Huang, Y., Zhang, Y., Hua, Y. and Wu, C. (2001). A new focal adhesion protein that interacts with integrin-linked kinase and regulates cell adhesion and spreading. *J. Cell Biol.* **153**, 585-598.

Uehata, M., Ishizaki, T., Satoh, H., Ono, T., Kawahara, T., Morishita, T., Tamakawa, H., Yamagami, K., Inui, J., Maekawa, M. et al. (1997). Calcium sensitization of smooth muscle mediated by a Rho-associated protein kinase in hypertension. *Nature* **389**, 990-994.

White, D. E., Coutu, P., Shi, Y. F., Tardif, J. C., Nattel, S., St Arnaud, R., Dedhar, S. and Muller, W. J. (2006). Targeted ablation of ILK from the murine heart results in dilated cardiomyopathy and spontaneous heart failure. *Genes Dev.* **20**, 2355-2360.

Wipff, P. J., Rifkin, D. B., Meister, J. J. and Hinz, B. (2007). Myofibroblast contraction activates latent TGF-beta1 from the extracellular matrix. *J. Cell Biol.* **179**, 1311-1323.

Yamaji, S., Suzuki, A., Sugiyama, Y., Koide, Y., Yoshida, M., Kanamori, H., Mohri, H., Ohno, S. and Ishigatsubo, Y. (2001). A novel integrin-linked kinase-binding protein, affixin, is involved in the early stage of cell-substrate interaction. *J. Cell Biol.* **153**, 1251-1264.

Yamazaki, T., Masuda, J., Omori, T., Usui, R., Akiyama, H. and Maru, Y. (2009). EphA1 interacts with integrin-linked kinase and regulates cell morphology and motility. *J. Cell Sci.* **122**, 243-255.

Yang, L., Qiu, C. X., Ludlow, A., Ferguson, M. W. and Brunner, G. (1999). Active transforming growth factor-beta in wound repair: determination using a new assay. *Am. J. Pathol.* **154**, 105-111.

Yang, T., Mendoza-Londono, R., Lu, H., Tao, J., Keller, J., Jiang, M. M., Shah, R., Chen, Y., Bertin, T. K., Engin, F. et al. (2010). E-selectin ligand-1 regulates growth plate homeostasis in mice by inhibiting the intracellular processing and secretion of mature TGF-beta. *J. Clin. Invest.* **120**, 2474-2485.

Zervas, C. G., Gregory, S. L. and Brown, N. H. (2001). Drosophila integrin-linked kinase is required at sites of integrin adhesion to link the cytoskeleton to the plasma membrane. *J. Cell Biol.* **152**, 1007-1018.

Zhang, W., Wu, Y., Wu, C. and Gunst, S. J. (2007). Integrin-linked kinase regulates N-WASp-mediated actin polymerization and tension development in tracheal smooth muscle. *J. Biol. Chem.* **282**, 34568-34580.

Zhang, Y., Guo, L., Chen, K. and Wu, C. (2002). A critical role of the PINCH-integrin-linked kinase interaction in the regulation of cell shape change and migration. *J. Biol. Chem.* **277**, 318-326.

Zhang, Z. G., Bothe, I., Hirche, F., Zweers, M., Gullberg, D., Pfitzer, G., Krieg, T., Eckes, B. and Aumailley, M. (2006a). Interactions of primary fibroblasts and keratinocytes with extracellular matrix proteins: contribution of alpha2beta1 integrin. *J. Cell Sci.* **119**, 1886-1895.

Zhang, Z. G., Lambert, C. A., Servotte, S., Chometon, G., Eckes, B., Krieg, T., Lapiere, C. M., Nusgens, B. V. and Aumailley, M. (2006b). Effects of constitutively active GTPases on fibroblast behavior. *Cell. Mol. Life Sci.* **63**, 82-91.

Zheng, B., Zhang, Z., Black, C. M., de Crombrugghe, B. and Denton, C. P. (2002). Ligand-dependent genetic recombination in fibroblasts: a potentially powerful technique for investigating gene function in fibrosis. *Am. J. Pathol.* **160**, 1609-1617.

Zweers, M. C., Davidson, J. M., Pozzi, A., Hallinger, R., Janz, K., Quondamatteo, F., Leutgeb, B., Krieg, T. and Eckes, B. (2007). Integrin alpha2beta1 is required for regulation of murine wound angiogenesis but is dispensable for reepithelialization. *J. Invest. Dermatol.* **127**, 467-478.